

PULSED LASER DEPOSITION OF CHALCOGENIDE FILMS FOR NONLINEAR PHOTONIC APPLICATIONS

A. Zakery*

Department of Physics, College of Sciences, Shiraz University, Shiraz 71454, Iran

Nonlinear optical properties of $\text{Ge}_{33}\text{As}_{12}\text{Se}_{55}$ pulsed-laser-deposited (PLD) films are presented. Degenerate four-wave mixing and Z-scan techniques were used to obtain the nonlinear refractive index and absorption coefficient of germanium arsenic selenide films. $\text{Ge}_{33}\text{As}_{12}\text{Se}_{55}$ films are highly nonlinear, and hence are suitable for ultra-fast all-optical switching applications. We designed and simulated a nonlinear directional coupler switch in PLD films. Current status of device fabrication and nonlinear properties of PLD deposited chalcogenide films is also discussed.

(Received April 19, 2005; accepted May 26, 2005)

Keywords: Nonlinear photonic devices, PLD Chalcogenide films, All-optical switching, Chalcogenide films

1. Introduction

Chalcogenide glasses are low phonon energy materials and are transparent from the visible up to the infrared. They are potentially low loss for the 1.3-1.5 μm telecommunication window and show attractive properties as hosts for active rare-earth ions [1,2]. These glasses have been used and recommended in a large number of applications such as fiber amplifiers, diffraction gratings, optical switching and waveguide fabrication [3-7]. Different techniques such as vacuum evaporation, sputtering, and spin coating have been used to prepare thin films of these glasses. Recently however, the ultra fast laser ablation technique has been used to fabricate thin films of GaLaS glasses [8]. In a previous study optical properties of PLD arsenic sulfide films were analyzed [9-10]. We have used different techniques to analyze optical properties of PLD films of another composition i.e., $\text{Ge}_{33}\text{As}_{12}\text{Se}_{55}$ in the present work. By using PLD method and the photobleaching effect [11] of this material we can design a nonlinear directional coupler (NLDC) switch. By taking into account the two and three photon absorption we solve numerically the differential equation governing the two waveguides (bar and cross) of NLDC and study its switching behavior.

2. Experimental

2.1. Film deposition

Up to now, thermal evaporation and sputtering have been used to create the chalcogenide glass thin films. Vacuum-evaporated films were used to fabricate waveguides in a $\text{As-S}_x\text{-Se}_y$ system of glasses, while sputtered films prepared were rapidly annealed. A significant problem encountered with these films is associated with the need to anneal them before exposure for waveguide writing. In general, their thermal-expansion coefficient is much larger than common substrate materials such as fused silica, leading to cracking or film lift off during or after annealing, while rapid thermal annealing has proven a useful approach to minimize these problems, any deposition process that removes the need for annealing would have a significant advantage.

* Corresponding author: zakery@susc.ac.ir

The properties of chalcogenide glasses deposited using pulse laser deposition (PLD) using a high-repetition-rate picosecond-range laser pulses was shown [10]. A well known advantage of the PLD technique is that it can actually transfer the stoichiometry of a multi-component target to a film deposited on a substrate. In addition, PLD can result in bombardment of the substrate by relatively high-energy ions or neutrals, and this assists in densification of the film in a way analogous to the use of ion bombardment during thermal evaporation. A disadvantage of the conventional PLD process which uses high-energy ($\approx 1\text{J}$), low repetition-rate (10-100Hz) nano-second laser pulse, is the production of particulates that can lead to high scattering losses in the films. The problem of particulates produced by conventional PLD can be eliminated by using the ultra-fast PLD process that employs short ($\approx 50\text{ ps}$), low energy (μJ), high-repetition-rate ($10^5\text{-}10^8\text{ Hz}$) pulse trains [12].

$\text{Ge}_{33}\text{As}_{12}\text{Se}_{55}$ flats (AMTIR-1) prepared by Amorphous Materials, Inc., Garland, TX75042 were used as ablation targets. Films of 1-4 μm thickness were deposited onto fused silica substrates using the ultra-fast laser deposition method [12]. The GeAsSe films depositions, were performed using the second harmonic of a mode-locked Nd:YAG laser ($\lambda=532\text{ nm}$, $t_p=50\text{ ps}$). The mode-locked pulses were Q-switched with a repetition rate of 10-12 KHz in order to increase the peak power. Each q-switched train contained approximately 30 to 35 pulses separated by the time interval of $\approx 3.2\text{ ns}$, thus the laser generated $(3\text{-}3.5)\times 10^5$ pulses each second. The average pulse energy was $\approx 10\text{ }\mu\text{J}$. The laser beam was directed into a vacuum chamber pumped to 3×10^{-7} Torr, and focused on a target with a special telecentric scanning lens, providing intensity up to $5\times 10^{10}\text{ W/cm}^2$ on the target surface. The deposition rate at a target-substrate distance of 150 mm was $2\text{ }\text{\AA}/\text{sec}$. The film composition was determined by the scanning electron microscopy (SEM), which allows quantitative and qualitative elemental mapping of the laser deposited films. The target composition was accurate to within $\approx 1\%$ while film composition differed from the source by up to $\approx 3.5\%$. The composition obtained for the film was $\text{Ge}_{29.5}\text{As}_{12.3}\text{Se}_{58.2}$. As is evident the atomic percentage of arsenic has remained approximately constant while the film was deficient in germanium and rich in selenium. It should be noted here that the composition $\text{Ge}_{33}\text{As}_{12}\text{Se}_{55}$ is used for the film throughout the paper.

2.2. Measurements of nonlinear optical constants

2.2.1. Degenerate four wave-mixing (DFWM) measurements

Nonlinear measurements were performed at 800 nm with 100 fs pulses from an amplified Ti: sapphire system. The measurements of DWFM were performed with a boxcar (forward) geometry [13]. For measurements on thin films we usually monitored two signals, one that was generated as the result of phase-matched interaction of the three incident beams and another of the non-phase matched signals generated by the chalcogenide film.

2.2.2. Z-Scan measurements

The Z-Scan measurements were performed on germanium arsenic selenide films of 2 μm thickness. 100-fs pulses with energies in the range of 0.1-0.5 μJ were used. In most measurements the focused spot size was in the range of $\omega_0=20\text{-}40\text{ }\mu\text{m}$, which resulted in the maximum light intensities in the range of 10-150 GW/cm^2 . A simple arrangement allowed us to record the open-aperture Z scan and the closed-aperture Z scan simultaneously. The Z scans obtained were analyzed with expressions derived by Sheik-Bahae et al. [14] to yield the real part of the nonlinear phase shift $\Delta\phi_{\text{real}}$ induced by the third-order nonlinearity and the T_t factor (defined here as $T_t = 4\pi\Delta\phi_{\text{imag.}}/\Delta\phi_{\text{real}}$) or a given sample. We performed this analysis by comparing the shapes of closed- and open-apertures scans with those computed theoretically. Roughly speaking, the amplitude of a closed aperture Z scan (i.e., the peak to the valley difference in transmission values) is proportional to the real part of the nonlinear phase shift $\Delta\phi_{\text{real}}$, whereas the asymmetry of a closed aperture scan depends on the T_t factor (for $T_t=0$ the scan is essentially S shaped and symmetric). The imaginary part of the nonlinear phase shift $\Delta\phi_{\text{imag}}$ can be obtained either from the asymmetry of the closed-aperture scan (with $\Delta\phi_{\text{imag.}} = \Delta\phi_{\text{real.}}/4\pi$) or from the depth of a dip in the open aperture scan that is directly related to the value of $\Delta\phi_{\text{imag.}}$.

3. Results

3.1. DFWM results

Fig. 1 shows a typical time-resolved DFWM curve obtained for a thin film of 2 μm thicknesses. It is evident that the signal has at least two components: the fast component corresponding to the laser pulse duration and a delayed component responsible for the tail in the temporal dependence of the signal. Because of the saturation behavior of the DFWM response we always verified that the DFWM data taken for the calculation of the values of n_2 were obtained at intensities low enough that we could assume Kerr-like behavior.

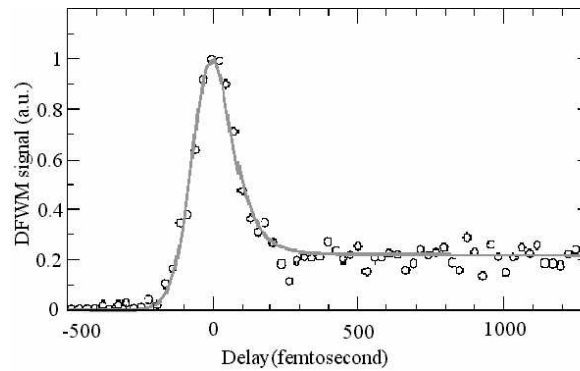


Fig. 1. DFWM signal from a 2 μm thick film of $\text{Ge}_{33}\text{As}_{12}\text{Se}_{55}$ at the total intensity of about 50 W/cm^2 . The experimental points (circles) are compared with a theoretical curve for a DFWM signal consisting of a fast response and a delayed response with the relaxation time of 100 picoseconds. The laser pulse duration is 105 femtoseconds. The nonlinearity determined from the DFWM result by calibrating against the signal from silica is $n_2 = 2 \times 10^{-13} \text{ cm}^2/\text{W}$

Equations describing DFWM predicts that, for negligible depletion of the pump beams, the intensity of the DFWM signal should be given by [13]:

$$I_{\text{DFWM}} = \text{const} |n_2|^2 L^2 I^3 \quad (1)$$

where n_2 is the non-linear refractive index, L is the film thickness and I is the total input intensity. If we use the above equation for the case of a germanium arsenic selenide film and also for the case of a fused silica substrate the following equation can be obtained and used to calculate the non-linear value of the refractive index for the germanium arsenic selenide film:

$$|n_2| = C_{\text{ref}} C_{\text{abs}} n_2^{\text{silica}} \frac{L_{\text{silica}}}{L_{\text{chalco}}} \left(\frac{I_{\text{DFWM}}^{\text{chalco}}}{I_{\text{DFWM}}^{\text{silica}}} \right)^{1/2} \quad (2)$$

where C_{ref} and C_{abs} are correction factors taking into account the differences in the reflection and absorption losses for the film and the fused silica substrate respectively. Actually the correction for the absorption is not very important to consider because both chalcogenide film and the fused silica substrate are almost transparent at the measurement wavelength (800 nm) but the reflection correction factor is more important. Due to the difference in their refractive indices at 800 nm, the reflection coefficient of the chalcogenide film could be as high as five times of the fused silica substrate of similar thickness. Hence some correction factor should be taken into account in this case. Our results were not corrected for reflection losses. The modulus of n_2 found from the above equation was $2 \times 10^{-13} \text{ cm}^2/\text{W}$.

3.2. Z-scan results

Fig. 2 shows examples of closed- and open-apertures scans for a germanium arsenic selenide film.

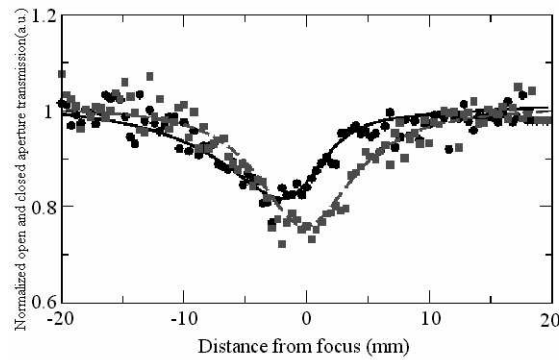


Fig. 2. Open (squares) and closed (circles) aperture Z-scan results obtained on a $2\ \mu\text{m}$ $\text{Ge}_{33}\text{As}_{12}\text{Se}_{55}$ film on a 1 mm silica substrate. The lines are results of numerical fitting. $\omega_0=32\ \mu\text{m}$, $\text{Re}(\Delta\phi)=0.36\ \text{rd}$, $T_1=12$. The results show that the nonlinear response of GeAsSe is dominated by an induced absorption effect. By calibrating the Z-scans against silica one can calculate the real and imaginary parts of the nonlinearity. The real part of the nonlinearity is approximately $\text{Re}(n_2) = 2.2 \times 10^{-13}\ \text{cm}^2/\text{W}$ and the imaginary part of the nonlinearity is characterized by a nonlinear absorption coefficient $\beta_2=5.6 \times 10^{-8}\ \text{cm}/\text{W}$.

The relation between the nonlinear phase shift and the nonlinear refractive index can be written as:

$$\Delta\phi = 2\pi n_2 I L_{\text{eff}} / \lambda \quad (3)$$

Where L_{eff} is an effective sample thickness (e.g. corrected for one-photon absorption, $L_{\text{eff}} = (1 - e^{-\alpha L})/\alpha$ and α is the linear absorption coefficient). Knowledge of the light intensity can be used for conversion from phase shift values to the nonlinearity values. It is, however, more convenient to perform the measurements in a relative manner. We therefore calibrated the values of the NLO parameters by performing measurements of the nonlinear phase shift for a fused silica plate for which $n_2 = 2 \times 10^{-16}\ \text{cm}^2/\text{W}$ was assumed. The thickness of the fused silica substrate was 1mm. The sign of n_2 deduced from Z-scan measurements was positive. Our results show that the nonlinear response of $\text{Ge}_{33}\ \text{As}_{12}\ \text{Se}_{55}$ is dominated by an induced absorption effect. The real part of the nonlinearity is appr. $\text{Re}(n_2) = 2.2 \times 10^{-13}\ \text{cm}^2/\text{W}$ and its imaginary part is characterized by a nonlinear absorption coefficient $\beta_2 = 5.6 \times 10^{-8}\ \text{cm}/\text{W}$.

3.3. Modeling of a NLDC switch

The demands for higher-data rate communication systems are stimulating research into new techniques for enhancing the capabilities of tomorrow's systems. Although wavelength-division-multiplexing techniques show great promise for upgrading existing systems, there is a simultaneous effort focused on enhancing system functionality and network flexibility through the use of fast optical switching and signal-processing techniques, and recent multi-Terabit transmission demonstrations have involved both wavelength- and time-division multiplexed systems. Fast switching on the timescale of picoseconds cannot be performed with electronic devices and researchers are investigating the use of all-optical components for ultra-fast operations such as switching, and time-division multiplexing and demultiplexing.

The requirement for operating times to be significantly faster than those possible with electronics means these optical components must operate in the picosecond or sub-picosecond range.

Compact devices will require large optical nonlinearities, so that switching can be effected at modest power levels. Another desirable feature relates to the integrability of these ultra-fast switching components with other optoelectronic components such as lasers and detectors. Although normal III-V semiconductor materials exhibit large optical nonlinearities near the band edge, they have a relatively slow (nanosecond) response due to slow recombination times for the optically-excited carriers.

The small size of these switching elements, combined with their integrability and low power requirements, provide considerable promise for practical applications.

The potential applications of nonlinear directional couplers (NLDC) in all optical processing have attracted a great deal of research since they first were introduced by Jensen in 1982 [15]. Usually these devices can be used as optical switches, optical limiters and logic gates. When they are used as switching devices NLDC can be self switching devices. A directional coupler consists of two identical single mode waveguides (bar and cross) placed in closed proximity to permit coupling between the evanescent fields. It is well known that a two waveguide NLDC with suitable length behaves as an optical switch. For use as a self-switch device couplers with Kerr nonlinearity are considered. When the optical power in a directional coupler is high enough that the nonlinearity in the coupler becomes important, power switching between the two waveguides becomes dependent on optical power.

Chalcogenide glasses have ultra-fast response time, low linear and nonlinear losses, high nonlinear Kerr coefficients, low noise and straightforward manufacturing with existing planar waveguide technology [4]. Hence they are a good candidate for making all optical switches especially NLDC switches. By depositing chalcogenide glass thin films on silica substrates using pulsed laser deposition (PLD) channel single mode waveguide [16] have been fabricated. Waveguides can also be written directly by means of selective photo-bleaching the chalcogenide film (by illumination the material with above band-gap light). Normally illumination of chalcogenide glasses with above band gap light causes photo-darkening to occur in these glasses. In the case of GeAsSe however, photo-bleaching occurs as a result of glass illumination. Illuminated areas have lower refractive indices and can be used as cladding for the waveguide. Finally by means of two such waveguides parallel and near each other a nonlinear directional coupler (NLDC) is constructed. By using the nonlinear properties of chalcogenide film we study the switching characteristic of NLDC. We use exactly the same equation used by Yang, Villeneuve, and Stegeman [17] but in our work we consider both two and three photon absorption mechanisms and neglect group-velocity dispersion and free carrier absorption. The equation governing the complex amplitude in the two waveguides of NLDC A_1 and A_2 are given by [17].

$$i \frac{\partial A_{1,2}}{\partial z} + \frac{2\pi a_2 n_2}{\lambda} \left(1 + \frac{iT}{8\pi} \right) |A_{1,2}|^2 A_{1,2} + \frac{i\beta_3 a_3}{2} |A_{1,2}|^4 A_{1,2} + KA_{2,1} = 0 \quad (4)$$

Here z, λ, K are the propagation coordinate, wavelength and linear coupling coefficient, respectively. The 2PA figure of merit T is given by $T = 2\beta_2 \lambda / n_2$ and n_2, β_2, β_3 are the nonlinear refractive index, 2 PA, and 3PA coefficients, respectively. a_2 and a_3 represent overlap integrals over the modal profiles in the waveguides for the third and fifth order nonlinearities, respectively. By using the normalized parameters $\zeta = z/L_c$ and $q_{1,2} = (2\pi a_2 n_2 L_c / \lambda)^{1/2}$, with $L_c = \pi/2K$ representing one half beat length, Equation (4) becomes

$$i \frac{\partial q_{1,2}}{\partial \zeta} + \left(1 + \frac{iT}{8\pi} \right) |q_{1,2}|^2 q_{1,2} + \frac{iV}{8\pi} |q_{1,2}|^4 q_{1,2} + \frac{\pi}{2} q_{2,1} = 0 \quad (5)$$

Here $V = I_c \lambda \beta_3 a_3 / (a_2 n_2)$, I_c being the cw critical intensity for switching given by $\lambda / (a_2 n_2 L_c)$. In equation (5) V is figure of merit associated with 3PA, which is related not only to the material parameters (n_2 and β_3) but also to device design. Effect of 3PA on switching operation was widely

studied in [17] and in the absence of 2PA, V must be smaller than 0.68. Fortunately the 3PA in chalcogenide glasses is very low but not ignorable [16], especially at high input powers. Because V is also design dependent a suitable value would be $V=0.1$ [17]. From our experimental results on chalcogenide films prepared by PLD we obtain $T=0.2$. By using this parameter we study the NLDC switch. Suppose the input power (P_{in}) enters the bar state of NLDC. We study the switching behavior by solving numerically coupled differential equations (5) and used a Runge-Kutta method by taking into account two and three photon absorption coefficients. Fig. 3 plots normalized output power (fraction of the output power to the input power) from the bar state versus normalized distance for various input powers. For comparison with the actual value ($T=0.2$ and $V=0.1$) that we chose from experimental data we also plotted normalized output power in the ideal case ($T=0$ and $V=0$ means two and three photon absorption are zero).

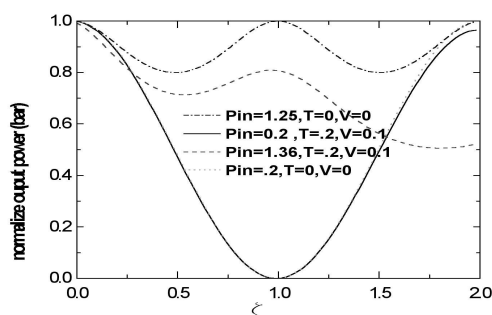


Fig. 3. Normalized output power from the bar state versus normalized distance for various normalized input powers. For low input powers and at half beat length ($\zeta = 1$) all of the power is in the cross state and for high input powers output power goes only into the bar state.

In Fig. 3 for the ideal case complete switching occurs at half-beat-length ($\zeta = 1$) which means that at half-beat-length for low input powers, output power from the bar state is zero while for high input powers, the output power from the bar state is %100 of the input power. This shows that the NLDC at half beat length behaves as a self switch. On the other hand in the same figure (Fig. 3) for the actual case ($T=0.2$ and $V=0.1$) at half-beat-length there is no difference between the ideal and actual cases when input power is low but for high input powers the role of two and three photon absorption affects the output power and reduces it to %80 of the input power. This result shows that although operation of the switch is not complete but switching occurs and is good enough.

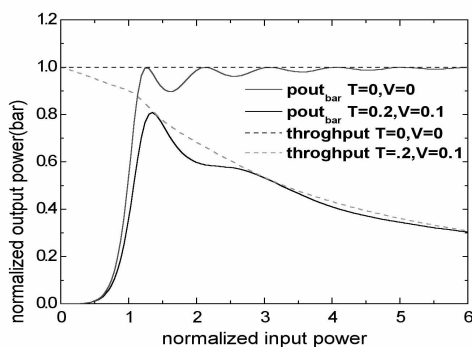


Fig. 4. Normalized output power (with respect to normalized input power) in the bar state and throughput (sum of normalized output powers from the bar and cross states) versus normalized input power at half-beat-length for the actual (lower curves) and ideal cases (upper curves).

For a more complete study of the switching behavior we plotted normalized output power in the bar state versus the input power at half beat length in the ideal and actual cases. As we see in Fig. 4 by increasing the normalized input power the normalized output power in the bar state also increases until it reaches the maximum normalized output power as expected. For the ideal case the maximum output power was %100 and for the actual case it was %80. An important point in Fig. 4 to note is that the maximum output power does not occur at the same normalized input power for the ideal and actual cases. For the ideal case the first maximum occurs at 1.25 but for the actual case it increases to 1.36 times of the normalized input power.

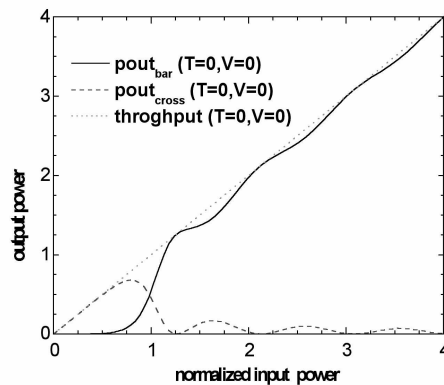


Fig. 5. Output power in the bar state and throughput (sum of output powers from the bar and cross states) versus normalized cw input power at half-beat-length for the ideal case. For low input power the output power in the bar state is very nearly proportional to input power.

After the first maximum in the ideal case we have another maximum which suggests that the switching can occur at higher normalized input powers but for the actual case we have only one maximum after the first maximum and throughput decreases and switching does not occur above 1.36 times of normalized input power.

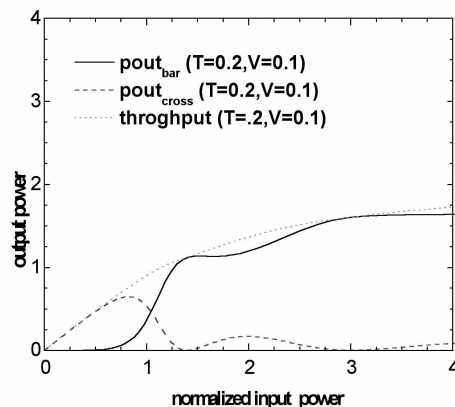


Fig. 6. Output power in the cross state and throughput (sum of output powers from the bar and cross states) versus normalized cw input power at half-beat-length for the actual case. For low input powers the output power from the cross state is proportional to input power. For high input powers contrary to the ideal case the output power remains constant.

Figs. 5 and 6 are similar to Fig. 4 but we plotted output power (not normalized with respect to the input power) for the ideal and actual cases at half-beat-length respectively. We see the behavior of the switch at low powers and also we observe that switching occurs at a normalized input power of 1.25 for the ideal and of 1.36 for the actual case. Also we see that in the ideal case for

input powers above 1.25 switching occurs and the output power is the same as the input power. For the actual case for powers above 1.36 we observe that the output power remains roughly constant which suggests that with increasing the input power the output power does not change and hence the input power does not affect the output power. This result may be used in other applications.

We have also modeled the behavior of the nonlinear directional switch by taking into account the group velocity dispersion GVD. If we consider the problem of pulse propagation by taking into account the group velocity dispersion (GVD), an equation of the form below is obtained which can be solved using the FSAT method [18].

$$i \frac{\partial q_{1,2}}{\partial \zeta} - H \frac{\partial^2 q_{1,2}}{\partial t'^2} + \left(1 + \frac{i\Gamma}{8\pi}\right) |q_{1,2}|^2 q_{1,2} + \frac{iV}{8\pi} |q_{1,2}|^4 q_{1,2} + \frac{\pi}{2} q_{2,1} = 0 \tag{6}$$

$$H = B_2 \pi / 4K$$

$$t' = t - z / v_g$$

In eq. (6) v_g is the group velocity, t is time, B_2 is GVD and K is usual coupling coefficient as previously defined. For the ideal case where two and three photon absorption coefficients are zero, the switch performance is studied when an input pulse is entered the bar state. As Fig. 7 shows, for pulses with low input intensities in the bar state, the performance of the switch is complete and efficient coupling is taking place. The effect of GVD is to broaden the pulse as expected.

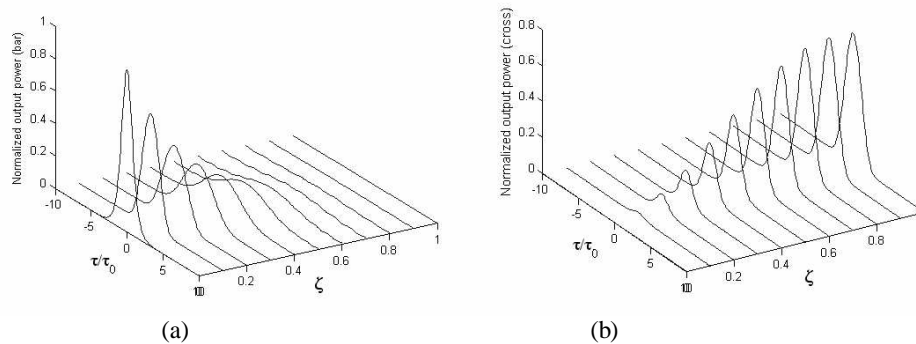


Fig. 7. Normalized output power for pulse propagation in (a) bar state (b) cross state of NLDC versus normalized distance ζ for low input intensities in the bar state. $H=1$ and $A=3$.

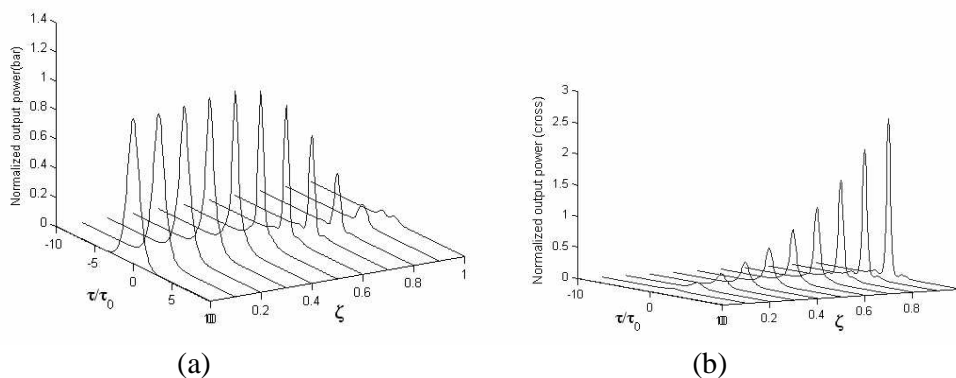


Fig. 8. Normalized output power for pulse propagation in (a) bar state (b) cross state of NLDC versus normalized distance ζ for medium input intensities in the bar state. $H=1$ and $A=2$.

For higher input pulse intensities, i.e., Fig. 8 and for the case of $A=2$, switching is still taking place but high nonlinearity starts to show its effect by narrowing of the pulse as is seen at long enough ζ . If we increase the input pulse intensity still further, as seen in Fig. 9, although the

switching is still taking place, its performance is not satisfactory. The pulse shape changes and is chirped, moreover, higher nonlinearities leads to narrowing of the pulse still further. It seems that if some higher GVD can be tolerated, a good performance of the switch can be expected even at high input pulse intensities.

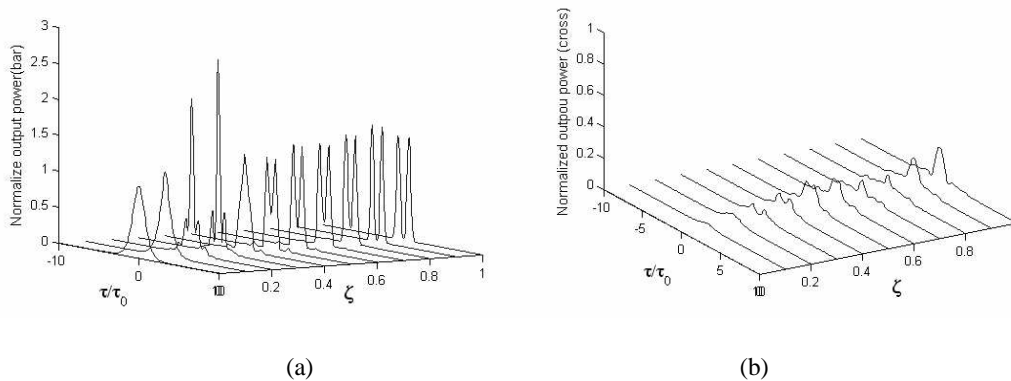


Fig. 9. Normalized output power for pulse propagation in (a) bar state (b) cross state of NLDC versus normalized distance ζ for high input intensities in the bar state. $H=1$ and $A=4$.

4. Discussion

4.1. Current status of nonlinear properties and device fabrication

4.1.1. Nonlinear properties

Fabrication and characterization of low loss rib chalcogenide waveguides was achieved [19]. To test the nonlinear properties of the chalcogenide waveguides they Measured spectral broadening due to self-phase modulation for pulses propagating through a 50 mm long and 5 μm waveguide. They showed that a 8 ps duration input pulses at 1573 nm were nearly transform-limited and were obtained from a KTP optical parametric oscillator (OPO). The power from the OPO was coupled into a SMF-28 single-mode fiber with a 3 mm long section of high NA fiber thermally expanded and spliced to its output end. The use of this short length of high NA fiber allowed high peak power to be delivered to the chalcogenide waveguide without any fiber-induced phase shift. A standard SMF-28 fiber was employed to collect a small fraction of the transmitted light and couple it to an optical spectrum analyzer. The measured spectrum broadening indicated that a phase shift of $\approx \pi$ was obtained [20]. The peak pulse power in the waveguide was obtained from the high NA fiber after correction of the coupling loss (about 1.8 dB/cm for one end) and waveguide loss, and was estimated to be 40 W. The effective area of the fundamental mode of the waveguide was modeled and found to be about 8 μm^2 . The calculated third order-nonlinearity based on the nonlinear phase shift was $3.05 \times 10^{-18} \text{ m}^2/\text{W}$, very close to the value of $2.92 \times 10^{-18} \text{ m}^2/\text{W}$ measured by Z-scan technique for bulk samples of the glasses [21]. It should be noted that the Z-scan for As_2S_3 indicates that the nonlinear figure of merit ($T = \beta\lambda/n_2$ where β is the two-photon absorption coefficient) is < 0.1 at 1550 nm. It is consistent with data of [22] where $T=0.009$ and hence two-photon absorption is expected to be negligible in these experiments [23]. They conclude that sub-watt switching can be achieved in a 5 cm long structure, assuming that the coupling loss can be held < 1 dB.

Gopinath et al. [24] have studied the third order optical nonlinearities of $\text{Ge}_{35}\text{As}_{15}\text{Se}_{50}$ with a glass transition temperature of 380 $^\circ\text{C}$. These glasses offer the potential for integration with traditional compound oxide glasses into highly nonlinear, high-index contrast fibers. They used Z-scan and femtosecond pump-probe techniques to measure the nonlinear refractive index and two-photon absorption coefficient of the glasses at telecommunication wavelengths. Nonlinearities as high as $\approx 900 \times$ that of silica were measured at 1540 nm.

A combination of pump-probe and Z-scan measurements allowed determination of the two-photon absorption coefficients of the chalcogenide glasses studied. The two-photon absorption coefficient β was measured to be $0.4 \text{ cm/Gw} \pm 25 \%$. Data was taken with intensities as high as 170 MW/cm^2 and no damage to the sample was observed.

A powerful but simple technique [25] based on a 4f coherent image system with top-hat beams was used to characterize nonlinear optical properties. They showed that, as in the Z-scan technique, the use of top-hat beams instead of Gaussian beams increases the sensitivity of the measurement. Intensity-dependent nonlinearities can be studied by use of this single laser-shot technique. They validated this nonlinear imaging technique by measuring the absolute value of n_2 coefficient for CS_2 and some well known chalcogenide glasses (As_2S_3 , As_2Se_3 , GeSe_3 , GeSe_4 and $\text{Ge}_{10}\text{As}_{10}\text{Se}_{80}$). Their values are in good agreement with those obtained by other techniques. The optical alignment is easy compared with the Mach-Zehnder technique. No displacement of the material is needed, unlike in the Z-scan method. Only one single laser shot is required, giving the possibility of studying materials showing intensity dependent n_2 . This is particularly advantageous in situations in which the optical beam quality of the laser output is poor (such as in optical parametric generator lasers).

The nonlinear refraction and absorption were measured by the Z-scan method at $1.05 \mu\text{m}$ [26]. The addition of Ag to As_2Se_3 glass led to an increase in the nonlinear refractive index without introducing an increase in the nonlinear absorption coefficient. The glass with a Ag content of 20 at. % revealed high nonlinearity ranging from 2000 to 27000 times that of fused silica, depending on the incident optical intensity. Although figure of merit of the samples tested at $1.05 \mu\text{m}$ does not satisfy a standard criterion ($T = \beta\lambda/n_2 < 1$), it can be expected to decrease at telecommunication wavelengths of 1.3 and $1.55 \mu\text{m}$. They believe that the Ag-As-Se glass is one of the most promising materials for all-optical switching devices at $1.55 \mu\text{m}$.

Ganeev et al. [27] investigated the nonlinear optical characteristics and the optical limiting in As_2S_3 , $\text{As}_{20}\text{S}_{80}$, $2\text{As}_2\text{S}_3/\text{As}_2\text{Se}_3$ and $32\text{As}_2\text{S}_3/\text{As}_2\text{Se}_3$ chalcogenide films. The nonlinear refractive indices and the two photon absorption coefficients of these films were measured using the Z-scan technique at wavelengths of a picosecond Nd:YAG laser ($\lambda=1064$ and 532 nm). The optical limiting associated with the Kerr-type nonlinearities was analyzed for the amorphous chalcogenide films. It was demonstrated that the $2\text{As}_2\text{S}_3/\text{As}_2\text{Se}_3$ film is characterized by a 12.5 fold optical limiting. The optical limiting due to two-photon absorption was investigated experimentally. It was found that the As_2S_3 film exhibits a 25-fold optical limiting.

Harbold et al. [28] have synthesized a series of chalcogenide glasses for the As-S-Se system that is designed to have strong nonlinearities. Measurements reveal that many of these glasses offer optical Kerr nonlinearities greater than 400 times that of silica at 1.25 and $1.55 \mu\text{m}$ and figures of merit for all-optical switching greater than 5 ($F = n_2/\beta\lambda$) at $1.55 \mu\text{m}$ were obtained.

Qiu et al. [29] report on photo-induced second-harmonic generation in chalcogenide glasses. Fundamental and second-harmonic waves from a nanosecond pulsed Nd:YAG laser were used to induce second-order nonlinearity in chalcogenide glasses. The magnitude of SHG in $\text{Ge}_{20}\text{As}_{20}\text{S}_{60}$ glass was 10^4 times larger than that of a telluride glass. Moreover, no apparent decay of photo-induced SHG in $\text{Ge}_{20}\text{As}_{20}\text{S}_{60}$ glass was observed after optical poling at room temperature. They suggest that the large and stable value of $\chi^{(2)}$ is due to the induced defect structures and large $\chi^{(3)}$ of the chalcogenide glasses.

The second-order nonlinear optical effects such as second harmonic generation (SHG) and linear electro-optics (LEO) in the middle infrared spectral range ($5\text{-}15 \mu\text{m}$) were experimentally observed [30] for the first time. They have found that the novel $\text{As}_2\text{Te}_3\text{-BaBr}_2\text{-BiCl}_2$ chalcogenide glasses, possessing transmission windows within the $3\text{-}45 \mu\text{m}$ spectral range, have both photo-induced SHG equal to 0.0012 pm/V and comparable values of photo-induced electro-optics effect at wavelength of excitation ($\lambda=10.6 \mu\text{m}$). The photo-induced anharmonic electron-phonon interaction play the major role in the observed phenomena. A good correlation between the IR-induced nonlinear optical susceptibilities and the photo-induced anharmonic electron-quasi-phonon interaction is demonstrated.

Meneghini et al. [31] have observed two-photon-induced refractive index changes in As_2S_3 thin films. This property is the key to creating self-written channel waveguides in a planar As_2S_3

slab. By exploiting the photosensitivity by exposure at 800 nm, where the penetration depth is large enough, they have induced the self-writing of channels in As_2S_3 thin-film waveguides. The waveguide formation is due to a permanent refractive-index increase induced by two-photon absorption. The channel evolution corresponds to that predicted by numerical simulations. Preliminary results show that a 1.55 μm beam is confined in the written channel.

Andriesh et al. [32] has described the nonlinear interaction of laser pulses with NS (noncrystalline semiconductors). It was found that these characteristics do not find a satisfactory explanation in the limits of the existing physical models proposed in the literature. A new mechanism of nonlinear light absorption in NS, taking into account the interaction with non-equilibrium phonons and localized vibrational modes is discussed briefly. It is not really difficult to estimate that the number of created phonons and localized vibrational modes due to the energy dissipation of hot carriers is of the same order of magnitude as the number of equilibrium phonons using a laser pulse energy density in the range 1-10 mJcm^{-2} . A reasonable agreement of the calculated results with the experimental ones was obtained. It was shown that PA (photo-induced absorption) can be observed in conditions of sub-bandgap excitation of thin films of chalcogenide glass by pump and probe light. PA arising during the short pulse excitation is explained by two-photon absorption. The slow component of PA was observed in the time regime longer than 10 ps after the stopping of excitation through the deep localized states. The peculiarities of PA in chalcogenide glass fibers are determined which could be explained by the model with multiple trapping of the carriers in localized states, distributed continuously in the gap.

4.1.2. Other Photonic devices

A number of chalcogenide rib waveguides with width ranging from 1 to 7 μm and depth from 0 to 4 μm were fabricated [19] using dry etching in As_2S_3 films prepared by the pulse laser deposition techniques. Propagation loss measurements were performed using the cut-back method using waveguides of lengths between 12 and 50 mm. A high quality polysiloxane coating ($n=1.53$) at 1.55 μm was applied to the top of waveguide as a cladding during characterization. The high index contrast ensured that light was tightly confined in the core layer. A high numerical aperture (NA) fiber with mode field diameter of 4.2 μm at 1.55 μm wavelength was used as input and output fiber to reduce the mode mismatch to the waveguides. Although the simulation showed that these deeply-etched waveguide structures supported multiple modes at 1.31 μm and 1.55 μm , higher order modes generally had high losses due to stronger coupling of the propagating field to the sidewalls. As a result only the fundamental mode was observed to propagate along these waveguides. The results of measurements of the transmission coefficient as a function of the length gave the smallest loss of 0.25 dB/cm at 1550 nm for the 4 and 5 μm wide waveguides, increasing to about 0.5 dB/cm for the 3 μm wide guides. This was due to the increased coupling of the fundamental mode to the sidewall as the waveguide became narrower. Se-based chalcogenide waveguides with similar dimensions were also characterized and higher loss (1.6 dB/cm) was however found at 1.55 μm .

Vallee et al. [33] have presented a real-time observation of Bragg grating formation in amorphous As_2S_3 ridge waveguides. Their experimental set up allowed them to monitor and control in situ the key parameters describing the Bragg diffraction, i.e., its reflectivity, resonant wavelength and FWHM. It was shown that the relatively small reflectivities of recorded Bragg gratings are not related to the small amplitude of refractive index modulation, which could be resulting from e.g., mechanical vibrations of their holographic set up. They have shown that the induced refractive index modulations in reality are large. Other detrimental factors such as multimode character of their channel waveguides and the spatial inhomogeneity of the induced refractive index changes in them actually prevented one to achieve higher grating reflectivities.

Low-loss shallow-rib waveguides were fabricated [34] using As_2Se_3 chalcogenide glass and polyamid-imide polymer. Waveguides were patterned directly in the As_2Se_3 layer by photo-darkening followed by selective wet etching. Theory predicted a modal effective area of 3.5-4 μm^2 , and this was supported by near-field modal measurements. The Fabry-Perot technique was used to estimate propagation losses as low as 0.25 dB/cm. First-order Bragg gratings near 1550 nm were holographically patterned in some waveguides. The Bragg gratings exhibited an index modulation on the order of 0.004. They were used as a means to assess the modal effective indices of the

waveguides. They assert that small core As_2Se_3 waveguides with embedded Bragg gratings have potential for realization of all-optical Kerr effect devices.

Nemec et al. [35] have studied the structure as well as thermally and optically induced effects in amorphous As_2Se_3 films prepared by pulse laser deposition. Amorphous films were prepared using rotating targets. KrF excimer laser operating at 248 nm with constant output energy of 300 mJ per pulse, with pulse duration of 30 ns and with repetition rate of 20 Hz was used for PLD of amorphous As-Se thin films. Raman spectra and optical properties (optical gap, refractive index, third-order non-linear susceptibility $\chi^{(3)}$) of prepared films and their photo-and thermally induced changes were studied. The structure of the laser deposited films was close to the corresponding bulk glasses contrary to thermal evaporated films. The composition of PLD films was practically unchanged during the process of deposition. They found that the optically and thermally induced changes of the refractive index and optical gap in PLD films are different from the changes occurring in thermally deposited films.

5. Conclusions

As our experimental results show, good-quality $\text{Ge}_{33}\text{As}_{12}\text{Se}_{55}$ films can be fabricated by the PLD technique. These films are highly nonlinear and a nonlinear refractive index $n_2=2.2 \times 10^{-13} \text{ cm}^2/\text{W}$ was obtained using a Z-scan technique. High nonlinearity of these films make them promising candidates for ultra-fast all-optical switching applications. The performance of a NLDC switch was studied and it was found that switching is taking place for the case of a cw input signal. In the case of pulse propagation, it was found however, that the performance of the switch is only satisfactory for low intensity input signals. Current status of fabrication of Rib and Ridge waveguides, Bragg gratings, as well as Optical limiters were discussed and their properties were presented. It was shown that Pulsed laser deposited chalcogenide films are suitable for fabrication of all-optical integrated circuits. Any future direction would be to enhance the nonlinearity still further. This would be achievable by somehow introducing suitable metal nano-particles in the glassy film.

Acknowledgement

The author would like to acknowledge M. Hatami for his help with numerical simulations in this work.

References

- [1] A. Bornstein, J. Flahaut, M. Guittard, S. Jaulmes, A. M. Loireau-Lozach, G. Lucazeau, R. Reisfeld, *The Rare Earths in Modern Science and Technology*, Ed. by G.J. McCarthy and J. J. Rhyne, Plenum, New York, p. 599. 1978.
- [2] T. Kanamori, Y. Terunuma, S. Takahashi, T. Miyashita, *J. Lightwave Technol.* **2**, 607 (1984).
- [3] M. Asoke, *Opt. Fiber. Technol. Mater. Devices Syst.* **3**, 142 (1997).
- [4] G. Lenz, J. Zimmermann, T. Katsufuji, M. E. Lines, H. Y. Hwang, S. Spalter, R. E. Slusher, S. W. Cheong, J. S. Sanghera, I. D. Aggarwal, *Opt. Lett.* **25**, 254 (2000).
- [5] C. W. Slinger, A. Zakery, P. J. S. Ewen, A. E. Owen, *Appl. Opt.* **1**, 2490 (1992).
- [6] J. F. Viens, C. Meneghini, A. Villeneuve, T. V. Galstian, E. J. Knystautas, M. A. Duguay, K. A. Richardson, T. Cardinal, *J. of Lightwave Technology* **17**, 1184 (1999).
- [7] S. Ramachandran, S. G. Bishop, *Appl. Phys. Lett.* **74**, 13 (1999).
- [8] K. E. Youden, T. Grevatt, R. W. Eason, H. N. Rutt, R. S. Deol, G. Wylangowski, *Appl. Phys. Lett.* **63**, 1601 (1993).
- [9] A. Zakery, *J. Phys. D: Appl. Phys.* **35**, 2909 (2002).
- [10] A. Zakery, Y. Ruan, A. V. Rode, M. Samoc, B. Luther-Davies, *J. Opt. Soc. Am. B* **20**, 1844 (2003).

- [11] A. Zakery, M. Hatami, *J. Opt. Soc. Am.* **B22**, No. 3/March (2005).
- [12] A.V. Rode, B. Luther-Davis, E. G. Gamaly, *J. Appl. Phys.* **85**, 4222 (1999).
- [13] F. P. Strohkendl, L. R. Dalton, R. W. Hellwarth, H. W. Sarkas, Z. H. Kafafi, *J. Opt. Soc. Am. B* **14**, 92 (1997).
- [14] M. Sheikh-Bahae, A. A. Said, T. Wei, D. J. Hagan, E. W. Van Stryland, *IEEE J. Quantum Electron.* **26**, 760 (1990).
- [15] M. Jensen S. M., *IEEE J. Quantum Electron.* **QE-18**, 1850 (1982).
- [16] A. Zakery, S. R. Elliott, *J. Non-Crys. Sol.* **330**, 1 (2003).
- [17] C. C. Yang, A. Villeneuve, G. I. Stegeman, *Opt. Lett.* **239**, 710 (1992).
- [18] H. Ghafouri-Shiraz, P. Shum, N. Nagata, *IEEE J. Quantum Electron.* **31**, 190(1995)
- [19] Y. Ruan, W. Li, R. Jarvis, N. Madsen, A. Rode, B. Luther-Davies, *Optics express* **12**, 5140 (2004).
- [20] G. P. Agrawal, in *nonlinear fiber optics*, Ed. by P.L. Kelley, I. P. Kaminow, G. P. Agrawal, Academic, 2001.
- [21] Y. Ruan, B. Luther-Davies, W. Li, A. Rode, M. Samoc, *ACTA Optica Sinica*, **23** (Supplement 363), 363 (2003).
- [22] M. Asobe, T. Kanamori, K. Naganuma, H. Itoh, *J. Appl. Phys.* **77**, 5518 (1995).
- [23] R. E. Slusher, B. J. Eggleton, in *nonlinear photonic crystals*, Ed. by R.E. Slusher and B. Eggleton, Springer, 2003.
- [24] J. T. Gopinath, M. Soljacic, E. P. Ippen, *J. Appl. Phys.* **96**, 6931 (2004).
- [25] S. Cherukulappurath, G. Boudebs, A. Monteil, *J. Opt. Soc. Am.* **B21**, 273 (2004).
- [26] K. Ogusu, J. Yamasaki, S. Maeda, M. Kitao, M. Minakata, *Optics Lett.* **29**, 265(2004).
- [27] R.A. Ganeev, A. I. Rysanyanski, T. Usmanov, *Physics of the solid state* **45**, 207 (2003).
- [28] J. M. Harbold, F. O. Ilday, F. W. Wise, J. S. Sanghera, V. Q. Nguyen, L. B. Shaw, I. D. Aggarwal, *Optics Lett.* **27**, 119 (2002).
- [29] J. Qiu, J. Si, K. Hirao, *Optics Lett.* **26**, 914 (2001).
- [30] I. V. Kityk, B. Sahraoui, *J. of Chem. Phys.* **114**, 8105- (2001).
- [31] C. Meneghini, A. Villeneuve, *J. Opt. Soc. Am.* **B15**, 2946 (1998).
- [32] A. Andriesh, V. Chumash, *Pure Appl. Opt.* **7**, 351 (1998).
- [33] R. Vallee, S. Frederick, K. Astaryan, M. Fischer, *Galstian, Opt. Communications* **230**, 301 (2004).
- [34] N. Ponnampalam, R. G. DeCorby, H. T. Nguyen, P. K. Dwivedi, C. J. Haugen, J. N. McMullin, S. O. Kasap, *Optics express* **12**, 6270(2004)
- [35] P. Nemeč, J. Jedelský, M. Frumar, M. Stabl, M. Vlček, *J. of Phys. and Chem. of Solids* **65**, 1253 (2004).